Tropical forcing of Circumpolar Deep Water Inflow and outlet glacier thinning in the Amundsen Sea Embayment, West Antarctica

E.J. STEIG[1], Q. DING[1], D.S. BATTISTI[2], A. JENKINS[3]*

[1]Department of Earth and Space Sciences and Quaternary Research Center, University of Washington, Seattle, WA, 98195, USA
[2]Department of Atmospheric Sciences, University of Washington, Seattle, WA, 98195, USA and the Geophysical Institute, University of Bergen, NO-5007 Bergen, Norway
[3]British Antarctic Survey, Natural Environment Research Council, High Cross, Madingley Road, Cambridge, CB3 0ET, UK

**To whom correspondence should be addressed: steig@uw.edu*

ABSTRACT. Outlet glaciers draining the Antarctic Ice Sheet into the Amundsen Sea Embayment (ASE) have accelerated in recent decades, most likely as a result of increased melting of their ice shelf termini by warm Circumpolar Deep Water (CDW). An ocean model forced with climate reanalysis data shows that, beginning in the early 1990s, an increase in westerly wind stress over the continental shelf edge drove an increase in CDW inflow onto the shelf. The change in local wind stress occurred predominantly in fall and early winter, associated with anomalous high sea level pressure (SLP) to the north of the ASE and an increase in sea surface temperature in the central tropical Pacific. The SLP change is associated with geopotential height anomalies in the middle and upper troposphere, characteristic of a stationary Rossby wave response to tropical SST forcing, rather than with changes in the zonally symmetric circulation. Tropical Pacific warming similar to that of the 1990s occurred in the 1940s, and thus is a candidate for initiating the current period of ASE glacier retreat. Further warming of the tropical Pacific can be expected to contribute to continued CDW inflow and continued melting of ASE outlet glaciers.

INTRODUCTION

Pine Island Glacier and Thwaites Glacier, the two largest of several fast-moving outlet glaciers that drain a large fraction of the West Antarctic Ice Sheet (WAIS) into the Amundsen Sea Embayment, have long been recognized as critical elements of WAIS dynamics (e.g. Lingle and Clarke, 1979). Hughes (1979; 1981) argued that it is these glaciers that make the WAIS most susceptible to large-scale collapse, which almost certainly occurred during some previous interglacial periods (Scherer and others, 1998; Pollard and DeConto, 2009; Naish and others, 2009). The inferred sensitivity of the Amundsen Sea Embayment (ASE) glaciers reflects of their bed geometry, which deepens inland (Lythe and others, 2001), the small size of the floating ice shelves at their termini, and the direct exposure of the ice shelves to the influence of warm, Circumpolar Deep Water (CDW) (Jacobs and others, 1996; Nitsche and others, 2007). In the mid-1990s it was discovered that melt rates under the Pine Island Glacier ice shelf are two orders of magnitude greater than under the much larger ice shelves in the Ross and Weddell Seas (Jacobs and others, 1996). Subsequent studies using satellite imagery and interferometry revealed that the grounding lines of Pine Island Glacier as well as Smith and Thwaites glaciers had retreated recently (Rignot, 1998; Rignot, 2001), that there was significant thinning well inland of the grounding lines (Wingham and others, 1998; Shepherd and others, 2002), and that glacier surface velocities were increasing (Joughin and others, 2003; Rignot, 2008).

Although the thinning of Amundsen Sea Embayment glaciers could in part reflect changes in surface mass balance (i.e. changes in snowfall in the drainage areas), Shepherd and others (2009) showed that the magnitude of thinning is too large to be explained that way, and that the pattern of changes is consistent with the diffusive upstream migration of a force perturbation beginning at the glacier bed (Schmelz and others, 2002, Payne and others, 2004). This in turn is consistent with a response to the thinning of the ice shelves (Shepherd and others, 2004) resulting from an increase in submarine melt rates due to enhanced delivery of heat from warm CDW, as had been suggested much earlier (Jacobs and others, 1992; 1996). These ideas were validated in 2010 by direct observations made by autonomous underwater vehicle under the Pine Island Glacier ice shelf, which mapped the subglacial topography in great detail, and measured water temperature, salinity, and oxygen content (Jenkins and others, 2010). These observations showed that CDW now floods the cavity below Pine Island Glacier, more than 30 km upstream of areas that were at least partially grounded as recently as the early 1970s. At several degrees above freezing, this CDW carries enough heat to be melting the ice from below at rates in excess of 50 m/year, in good agreement with estimates independently derived from the observed ice velocities and thinning rates (e.g. Rignot and others, 2008).

Thoma and others (2008) used a regional ice-ocean model to show that recent changes in the influx of CDW in the ASE could be attributed to changes in the frequency and strength of westerly winds over the edge of the continental shelf. The timing of modelled increases in CDW influx is similar to the timing of two distinct phases of acceleration on Pine Island Glacier, in 1974-1987 and after 1994, that were separated by a period of quiescence (Joughin and others, 2003; Rignot and others 2008; Scott and others, 2009; Wingham and others, 2009). Jenkins and others (2010) found that as of 1973, the grounding line of Pine Island Glacier had already retreated from the top of a subglacial topographic ridge, suggesting that the retreat throughout the observational record, as well as into the future, was likely to be an inevitable result of the well-known marine ice sheet instability associated with deepening of the seabed inland of the ridge crest (e.g. Schoof, 2007). This finding raised a question about the relative roles of contemporaneous ocean forcing and continuing ice sheet response to an earlier event in controlling the current behaviour of the glacier. However, Joughin and others (2010) suggest that subtle topographic highpoints on the otherwise downwards slope from the ridge crest could have halted grounding line retreat, at least temporarily, and that ocean forcing could have played a role in re-starting the retreat. Furthermore, not only Pine Island Glacier, but also Thwaites and Smith Glaciers thinned in the 1990s (Shepherd and others, 2002), and glaciers are thinning at present nearly everywhere along the Amundsen Sea margin of the WAIS despite varying bed geometry (e.g. Pritchard et al., 2009).

Thus, while the complex interaction between bed slope, glacier dynamics and ocean forcing remains to be fully understood, the evidence appears to be firm that changes in CDW inflow to the ASE, driven by changes in local wind forcing, have played a role in influencing the thinning and retreat of glaciers in the ASE. This raises the question of how the observed changes in winds in the ASE are related to larger-scale changes in atmospheric circulation. Thoma and others (2008) found that the correlation between local circulation in the ASE and commonly used indices of the large scale circulation, the Southern Annular Mode (SAM) index and the Southern Oscillation Index (SOI), was low. However, the causes of local wind changes cannot generally be ascribed to a single large-scale index, and the relevant dynamics probably depends on the season in which changes in CDW influx have occurred. In this paper, we explore the relationship between ASE winds, modelled CDW upwelling, and the large-scale circulation in more detail.

DATA AND METHODS

Thoma and others (2008) modelled CDW intrusions onto the ASE shelf using a regional ice-ocean model based on a version of the Miami Isopycnic Coordinate Ocean Model of Bleck and others (1992) adapted to include sub-ice-shelf cavities by Holland and Jenkins (2001). They forced the model with sea level pressure and sea surface temperature variations from the NCEP climate reanalysis data (Kalnay and others, 1996). We use their monthly model output of the thickness of CDW layers (isopycnic model layers 7 and 8) on the continental slope and on the inner shelf, near the margin of Pine Island Glacier, for the period 1980 through 2004. The continental shelf edge in the ASE region is oriented approximately east-west, and Thoma and others (2008) argued that increased westerlies would lead to enhanced CDW intrusion across the shelf. As a proxy for the westerlies they used a simple index for the geostrophic wind, based on the sea level pressure (SLP) difference north and south of the shelf edge. Here, we use the zonal wind stress over the shelf edge as a more direct measure of atmospheric forcing.

A simple explanation for the relationship between westerly wind stress and CDW inflow is the northward Ekman transport of surface waters that lifts CDW up the slope and drives it onto the outer shelf. While this process undoubtedly operates, the bulk of the inflow, which is focussed on the shelf-edge troughs, is driven by more complex interactions between the temporally varying shelf-edge currents and the spatially varying topography, and is probably related to both the overall strength and the variability of the westerly wind stress (Klinck and Dinniman, 2010). Once on the continental shelf, CDW is transported into Pine Island Bay by a combination of the cyclonic circulation on the shelf and the deepening of the seabed along the axes of the main glacial troughs (Nitsche and others, 2007). Strong statistical relationships between westerly wind stress and the modelled CDW response, including a reasonable lag time (implying mean currents of ~5-10 cm/s along the main trough that extends across the continental shelf towards Pine Island Glacier) show that seasonal mean westerly wind stress is a physically meaningful measure of the atmospheric dynamics relevant to CDW inflow.

To obtain wind stress data, and for analysis of the large-scale climate fields, we use both NCEP2 (Kanamitsu et al., 2002) and a combination of ERA40 (1979-2004) and ERA-interim (2005-2009) reanalysis products (Uppala et al., 2005). Following other recent work (Ding and others, 2011), in some figures we show ERA40/ERA-interim data only, but the results are not dependent on which product is used. While zonal wind stress changes could occur without changes in the zonal wind speed, the monthly zonal component of wind stress and wind speed are highly correlated in this region because the variability in the meridional wind is much weaker than in the zonal wind. The wind stress and the estimate of geostrophic wind used by Thoma and others (2008) are therefore closely comparable. We use daily and monthly wind stress at 70°S, averaged over 100° W to 125°W, corresponding to the continental slope at the edge of the ASE (Fig. 1).

RELATIONSHIP BETWEEN LOCAL WIND STRESS AND MODELLED CIRCUMPOLAR DEEP WATER INFLOW

In the climatological mean, westerly wind stress at the ASE shelf edge occurs predominantly in fall through spring, with a maximum in late winter (Fig. 1). In austral summer, the wind stress is weak easterly. The true seasonal variability of CDW intrusions in the ASE is not known, due to the very limited available data. However, the model results of Thoma and others (2008) show the greatest quantity of CDW on the outer shelf during spring, about one month after the climatological maximum in westerly wind stress, and a subsequent maximum on the inner shelf one to two months later. The lag between wind stress over the continental slope and modelled inner shelf CDW layer thickness is quite consistent (~2.5 months) on both seasonal and interannual timescales, as clearly seen in a simple lag correlation plot (Fig. 2a). A spectral coherence calculation suggests the same phase lag also extends to decadal timescales (Fig. 2b,c), though this cannot be demonstrated to be statistically significant.

In the early 1990s, there is a significant increase in the thickness of modelled CDW in the ASE (Figure 3), at least approximately coincident with the observation of resumed acceleration of Pine Island Glacier after 1994 (Joughin and others, 2003). This appears as a gradual increase beginning in the early 1990s, and a transition to a period of larger and more variable inner shelf layer thickness around 1994. Although the mean monthly westerly wind stress (Figure 1b) does not show such an obvious transition, there is a pronounced increase in austral fall and early winter in the early 1990s (March through June; Figure 4). Indeed, while the seasonal maximum wind stress remains in winter and spring, the westerly wind stress in fall more than doubles between the 1980s and 1990s (Figure 4). Importantly, the maximum layer thickness change between the 1980s and 1990s on the outer continental shelf also occurs in fall and early winter, and the maximum layer thickness change on the inner continental shelf occurs one to three months later (Figure 3), indistinguishable from the average phase lag seen for seasonal and interannual variability. Thus, the significant increase in modelled CDW inflow between the 1980s and 1990s is the result of a shift in atmospheric conditions occurring in fall and early winter.

RELATIONSHIP BETWEEN LOCAL WIND STRESS AND LARGE-SCALE ATMOSPHERIC CIRCULATION

We now turn to the causes of the observed variability and change in westerly wind stress in the ASE. The seasonal variations are well understood, and are associated with the development of a pattern of increased sea level pressure (SLP) immediately to the north of the ASE, a corresponding weakening of the low-pressure trough (Fig. 1) along the ASE coastline, and an eastward shift and contraction of the Amundsen Sea Low (e.g. van den Broeke, 2000; Simmonds and King, 2004). A similar pattern of variability also occurs on longer timescales, and various mechanisms have been proposed depending on the season involved. Two commonly used indices of atmospheric circulation relevant to Antarctic climate variability are the Southern Annular Mode (SAM) index (e.g. Marshall, 2006), which reflects the strength of the average circumpolar westerlies, and the Southern Oscillation Index (SOI; e.g. Trenberth, 1984), which reflects conditions in the tropical Pacific. Ding and others (2011) have shown that correlation between the SOI and Amundsen Sea climate is linked more to variability in sea surface temperature (SST) in the central tropical Pacific than in the eastern Pacific region that characterizes El Niño events. The Niño3.4 region (5°S-5°N, 190°-240°E) is a commonly used measure of central Pacific SST variability.

Table 1 shows the correlation between the zonal wind stress over the ASE shelf edge and various measures of large-scale climate variability as a function of season. Statistically significant correlations in summer (DJF) are found only with the SAM index. In winter (JJA) and spring (SON), statistically significant correlations are found with measures of tropical variability but not with the SAM index. In austral fall (MAM), significant correlations are found both with the SAM index and with central tropical Pacific and South Pacific Convergence Zone (SPCZ) SSTs, as well as with the SOI. In no season is there any significant correlation with the NOAA Antarctic Oscillation Index, an alterative measure of zonally symmetric SAM variability (e.g. Mo, 2000).

	Season					
	DJF	MAM	JJA	SON	Annual	AMJ
SAM Index	***0.34***	**0.35**	0.07	0.09	0.05	0.11
Antarctic Oscillation Index	0.12	0.24	0.04	-0.01	-0.01	-0.11
Southern Oscillation Index	0.20	**0.36**	0.31	**0.61**	**0.60**	**0.36**
Eastern Tropical Pacific SST	0.21	0.19	0.13	**0.35**	**0.36**	**0.43**
Central Tropical Pacific SST	0.19	**0.36**	***0.34***	**0.47**	**0.53**	0.20
Nino3.4 SST	0.20	0.33	**0.37**	**0.45**	**0.55**	**0.40**
SPCZ SST	0.14	**0.49**	0.14	0.26	**0.40**	0.33

Table 1. Correlations between zonal wind stress (ERA40/ERAintrim) along the shelf edge of the Amundsen Sea Embayment, and the SAM index, AAO index, SOI, and sea surface temperatures (SST) in the tropical and subtropical Pacific (ERSST3), for the period 1979-2009. Latitude and longitude ranges for the SSTs are as follows: Eastern: 6°S-6°N, 240°-280°E; Central: 6°S-6°N, 160°-240°E; Nino3.4: 6°S-6°N, 190°-240°E; SPCZ: 20°S-8°S, 180°-240°E. Bold numbers indicate significant correlation above the 95% level, italics at the >90% confidence level.

The seasonal differences in correlation patterns shown in Table 1 support previous work on the causes of variability in the Amundsen Sea region. Most studies of the SAM have focused on summer, during which significant decadal trends in the SAM have occurred, particularly between the 1980s and 1990s (e.g. Thompson and Solomon, 2002). There is no significant trend in the winter or spring SAM index in the last thirty years, but there are large changes observed in Amundsen sector sea ice and Antarctic surface temperatures in those seasons (Comiso and Nishio, 2008; Steig and others, 2009) that have been linked with changes in tropical Pacific SSTs (Ding and others, 2011; Schneider and others, 2011). Turner and others (2009) showed that recent trends in sea ice as well as changes in SLP and geopotential height in the Amundsen sector are significant in the fall in the last 30 years, and suggested that those changes – reminiscent of the climatological fall-to-winter change in the Amundsen Sea Low – could be explained by changes in the SAM. While this is consistent with our finding of a significant correlation between the fall SAM index and the ASE westerlies, this result is quite sensitive to the data set and season chosen: there is no correlation with the AAO index in any season, and in the late fall/early winter season (AMJ), there is no correlation with the SAM. In contrast, wind stress in MAM and AMJ is consistently as high or more highly correlated with indices of tropical variability than with the SAM.

Figure 5 shows maps of the correlation between ASE zonal wind stress and SLP, the upper troposphere streamfunction, ψ ($\mathbf{u} = \nabla\times\psi$, where $\mathbf{u}$ is the wind velocity), and SST for austral fall (MAM). The most prominent feature in SLP is a significant correlation in the Amundsen Sea sector of the Southern Ocean. The SLP anomalies are the surface expression of a deep coherent tropospheric circulation, with corresponding geopotential height anomalies in the middle and upper troposphere. The dynamical connection between ASE wind stress and the tropical Pacific is apparent in the correlation with the streamfunction at the 200 hPa level (Fig. 5b), which shows a sequence of positive and negative correlation centres extending from the central equatorial Pacific to the far south Pacific. These patterns, along with the nearly equivalent barotropic structure of the high latitude geopotential height anomalies, are characteristic of a stationary Rossby wave response to tropical SST forcing (e.g. Gill, 1980; Mo and Higgins, 1981; Hoskins and

Karoly, 1998). Correspondingly, the correlation between ASE westerly wind stress and SST features a positive SST anomaly in the central tropics, shown in Fig 5c.

The dynamics that are responsible for the teleconnection between the tropical Pacific and the south Pacific are well established (e.g. Sardeshmuhk and Hoskins 1988; Lachlan-Cope and Connolley, 2006): anomalously high SSTs in the central Pacific force an increase in tropical convection in regions of strong potential vorticity gradients (associated with the subtropical jet east of Australia), which creates a strong Rossby wave that propagates along a great-circle path towards the Amundsen Sea. Indeed, Ding et al. (2011) showed that modest positive tropical SST anomalies in the central Pacific, very similar in pattern to that shown in Fig. 5c, force atmospheric circulation anomalies consistent in pattern and amplitude with those shown in Fig. 5(a,b) – including in the Amundsen Sea.

The same physics that relates tropical SSTs with interannual anomalies in ASE zonal wind stress in MAM also appears to be responsible for the decadal changes in wind stress that account for the modelled changes in CDW layer thickness. Figure 6 shows the change in SLP, upper level stream function and SST between the 1980s and the 1990s that accompany the CDW layer thickness and wind stress changes shown in Fig. 3 and 4. The patterns of surface and upper level circulation and SST changes associated with the decadal changes in the ASE zonal winds are strikingly similar to the pattern of interannual correlations. Hence, it appears that tropical SST forcing is responsible for a significant fraction of both interannual variability and decade-to-decade change in ASE zonal wind stress. Tropical SST forcing thus plays an important role in influencing the amount of warm CDW that flows across the continental shelf to bathe the PIG ice shelf and the margins of other outlet glaciers in the Amundsen Sea Embayment.

DISCUSSION

The results above show that both interannual variability and longer term changes in westerly wind stress in the Amundsen Sea Embayment, relevant to forcing CDW inflow to the continental shelf, is significantly influenced by conditions in the tropics. In the annual mean, as much of 30% or more of the variance in zonal ASE wind stress can be attributed to tropical forcing, depending on which measure of tropical variability is used.

While regional, high latitude atmospheric processes obviously are also important – and must dominate the unforced variability – it is striking that only in the summer season does the SAM appear to play a role that is comparable with that of the tropical forcing. The largest changes in wind stress occur in fall and early winter, when tropical forcing is clearly dominant.

The distinction between low latitude versus high latitude forcing of the ASE wind stress has significant implications for our understanding of both recent and future changes in CDW inflow, and therefore to the past and future evolution of Pine Island Glacier and other outlet glaciers in the area. Recent changes in the SAM in summer have widely been attributed to radiative forcing resulting from the decline in stratospheric ozone (Thompson and Solomon, 2002). If changes in the ASE winds in fall were similarly attributed to ozone-related SAM changes, this would imply that as the ozone hole recovers over the next few decades, the current, apparently anomalous wind field pattern will change, implying a return to pre-1990s CDW inflow strength. The attribution of fall SAM changes to ozone forcing is problematic, however, because this would require a three to six-month lagged response to spring ozone depletion (e.g., Thomspon and Solomon 2002, Gillett and Thompson, 2003; Keeley and others 2004). Furthermore, the SAM index itself is not independent of tropical conditions: observations show, for example, that a positive SAM index is more likely to occur during a La Niña year (Fogt and Bromwich, 2006; Fogt and others, 2010). L'Heureux and Thompson (2006) concluded that about 25% of the interannual variability in the SAM can be attributed to El Niño-Southern Oscillation variability in austral summer, while Grassi and others (2005) show that the observed zonal SAM pattern change at 500 hPa geopotential heights between the 1980s and the 1990s can be simulated with an atmospheric general circulation model using observed tropical SST forcing alone. Fogt and Bromwich (2006) attributed the significant observed change in the expression of the SAM in the Amundsen Sea region between the 1980s and 1990s largely to the great number of El Niño and La Niña events during the latter decade. Thus, the role of tropical forcing is unequivocal.

CONCLUSIONS

Flow of warm CDW onto the continental shelf has played a critical role in the high melt rates and recent thinning and retreat of glaciers in the Amundsen Sea Embayment region of West Antarctica. Variability in CDW inflow is strongly influenced by the strength of the westerly wind stress over the continental slope, and tropical SST forcing has played an important, if not dominant role, in recent changes in the zonal wind regime in the ASE. Continued changes in tropical SSTs can be expected in the future, due to increased global radiative forcing from anthropogenic greenhouse gases, and warming in the central tropics is particularly pronounced in most AR4 model runs (Ding and others, 2011), suggesting that the current wind stress regime in the ASE is likely to persist. In this context, it is interesting to note that significantly anomalous warming in the central tropical Pacific last occurred in the 1940s, and ice core evidence indicates that it had a comparable impact on climate in the Amundsen Sea sector of Antarctica (Schneider and Steig, 2008). While the link from wind changes to CDW inflow changes to glacier retreat is obviously not a simple linear process, this nevertheless suggests that tropical SST forcing during the 1940s is a viable candidate for the initiation of the current period of change in the Amundsen Sea ice shelves, which clearly was underway at least by the 1970s. Photographic evidence (Rignot, 2002) shows that in 1947, the Pine Island Glacier ice shelf was only slightly more advanced than in the early 1970s, but that a large area of icebergs and sea ice extended seaward of the ice front suggesting the aftermath of a major calving event. Furthermore, there is independent evidence from sediment cores that a larger ice shelf occupied the ASE at some time prior to this (Kellogg and Kellogg, 1997). We speculate that a more extensive ice shelf may have partially collapsed following the very large El Niño/La Niña cycle of 1941-1943.

ACKNOWLEDGEMENTS: We thank Marcel Küttel, Spruce Schoenemann, Paul Hezel, Ed Blanchard-Wrigglesworth and Joe MacGregor for fruitful discussion. Mauri Pelto's summary of the history of studies of Pine Island Glacier at RealClimate.org provided useful background information. This manuscript stemmed in part from discussions at the 2010 session of the Advanced Climate Dynamics Courses, funded by the Norwegian Centre for International Cooperation in Higher Education, the University of Washington, the Massachusetts Institute of Technology, NASA and DoE. This research was supported by U.S. National Science Foundation grant number OPP-0837988 to EJS, a U.K. Natural Environment Research Council grant number NE/G001367/1 to AJ, and by the University of Washington's Quaternary Research Center.

REFERENCED CITED

Bleck, R., C. Rooth, D. Hu, and L. T. Smith. 1992. Salinity-driven thermo- cline transients in a wind- and thermohaline-forced isopycnic coordinate model of the North Atlantic, *J. Phys. Oceanogr.* 22(12), 1486–1505.

Comiso J.C. and Nishio. 2008. Trends in the sea ice cover using enhanced and compatible AMSR-E, SSM/ I, and SMMR data. *J. Geophys. Res.* 113:C02S07. doi:10.1029/2007JC420057.

Ding, Q., E.J. Steig, D.S. Battisti and M. Küttel. 2011. Winter warming in West Antarctica caused by central tropical Pacific warming. *Nature Geoscience* 4, 398–403.

Fogt, R.L. and D.H. Bromwich. 2006. Decadal Variability of the ENSO Teleconnection to the High-Latitude South Pacific Governed by Coupling with the Southern Annular Mode. *J. Climate* **19**, 979–997.

Fogt, R.L., D.H Bromwich and K.M. Hines. 2010. Understanding the SAM influence on the South Pacific ENSO teleconnection. *Clim. Dyn.* **36**, 1555–1576.

Gill, A. E. Some simple solutions for heat induced tropical circulation. 1980. *Q. J. R. Meteorol. Soc*. 106, 447–462.

Gillett, N. P. and D.W.J. Thompson. 2003. Simulation of recent Southern Hemisphere climate change. *Science* 302, 273–275.

Grassi, B., G. Redaelli, and G Visconti. 2005. Simulation of Polar Antarctic trends: Influence of tropical SST. *Geophys. Res. Lett*. **32** (23), doi:10.1029/2005GL023804.

Holland, D. M. and A. Jenkins. 2001. Adaptation of an isopycnic coordinate ocean model for the study of circulation beneath ice shelves. *Mon. Weather Rev*., 129(8), 1905–1927.

Hoskins, B. J. and D.J. Karoly 1981. The steady linear response of a spherical atmosphere to thermal and orographic forcing. *J. Atmos. Sci*. 38, 1179–1196.

Hughes, T.J. 1979. Reconstruction and disintegration of ice sheets for the CLIMAP: 18000 and 125000 years B.P. experiments: theory. *J. Glac.* 90, 493–495.

Hughes, T.J. 1981. The weak underbelly of the West Antarctic ice sheet. *J. Glac.*27, 518–525.

Jacobs, S. S., H. H. Hellmer, and A. Jenkins 1996. Antarctic ice sheet melting in the southeast Pacific. *Geophys. Res. Lett.*, 23(9), 957–960.

Jacobs, S. S., H. H. Hellmer, C. S. M. Doake, A. Jenkins and R. M. Frolich. 1992. Melting of ice shelves and the mass balance of Antarctica. *J. Glaciol.*, **38**(130), 375–387.

Jenkins, A., P. Dutrieux, S. S. Jacobs, S. D. McPhail, J. R. Perrett, A. T. Webb and D. White. 2010. Observations beneath Pine Island Glacier in West Antarctica and implications for its retreat. *Nature Geosci.*, **3**, 468–472, doi:10.1038/ngeo890.

Joughin, I., B. E. Smith, and D. M. Holland. 2010. Sensitivity of 21st century sea level to ocean-induced thinning of Pine Island Glacier, Antarctica. *Geophys. Res. Lett.* **37,** L20502.

Joughin, I., E. Rignot, C. E. Rosanova, B. K. Lucchitta, and J. Bohlander. 2003. Timing of recent accelerations of Pine Island Glacier, Antarctica. *Geophys. Res. Lett*. 30(13), 1706, doi:10.1029/2003GL017609.

Kalnay, E., et al. 1996. The NCEP/NCAR 40-year reanalysis project, *Bull. Am. Meteorol. Soc.*, 77(3), 437–471.
Kanamitsu, M. et al. 2002. NCEP-DOE AMIP-II Reanalysis (R-2). *Bull. Am. Meteorol. Soc*. 83, 1631–1643.
Keeley, S. P. E., N. P. Gillett, D. W. J. Thompson, S. Solomon and P. M. Forster. 2007. Is Antarctic climate most sensitive to ozone depletion in the middle or lower stratosphere? *Geophys. Res. Lett.*,34, L22812, doi:10.1029/2007GL031238.
Kellogg, T. B. and D.E. Kellogg. 1987. Recent glacial history and rapid ice stream retreat in the Amundsen Sea. *J.Geophys. Res*. 92, 8859–8864.
Klinck, J.M. and M.S. Dinniman. 2010. Exchange across the shelf break at high southern latitudes. *Ocean Sci*. 6, 513–524.
L'Heureux, M.L. and D.W.J. Thompson. Observed Relationships between the El Niño–Southern Oscillation and the Extratropical Zonal-Mean Circulation. *J. Climate* 19, 276–287 (2006).
Lachlan-Cope, T. and W. Connolley,. 2006. Teleconnections between the tropical Pacific and the Amundsen-Bellinghausens Sea: Role of the El Niño/Southern Oscillation. J. Geophys. Res. 111, D23101.
Lingle, C.S. and J.A. Clark. 1979. Antarctic ice-sheet volume at 18 000 years B.P. and Holocene sea-level changes at the West Antarctic margin. *Journal of Glaciology* 24, 213–230.
Lythe, M. B., D. G. Vaughan, and the BEDMAP Consortium. 2001. BED- MAP: A new ice thickness and subglacial topographic model of Antarctica, *J. Geophys. Res*. 106(B6), 11335–11351.
Marshall, G. 2003. Trends in the Southern Annular Mode from observations and reanalyses. *J. Climate* (2003).
Mo, K. C. 2000. Relationships between low-frequency variability in the Southern Hemisphere and sea surface temperature anomalies. *J. Climate* 13, 3599-3610.
Mo, K. C. and R.W. Higgins,1998. The Pacific–South American modes and tropical convection during the Southern Hemisphere winter. *Mon. Weath. Rev.* 126, 1581–1596.
Naish, T. and 55 others. 2009. Obliquity-paced Pliocene West Antarctic ice sheet oscillations. *Nature* 458, 322–328.
Nitsche, F. O., S. S. Jacobs, R. D. Larter, and K. Gohl. 2007. Bathymetry of the Amundsen Sea continental shelf: Implications for geology, oceanography, and glaciology. *Geochem. Geophys. Geosyst*. 8, Q10009, doi:10.1029/2007GC001694.
Payne, A. J., A. Vieli, A.P. Shepherd, D.J. Wingham and E. Rignot. 2004. Recent dramatic thinning of largest West Antarctic ice stream triggered by oceans. *Geophys. Res. Lett*. 31, L23401 (2004).
Pollard, D. and R.M. DeConto. 2009. Modelling West Antarctic ice sheet growth and collapse through the past five million years. *Nature*, 458(7236): 329-U89.
Pritchard, H., R.J. Arthern, D. Vaughan and L.A. Edward. 2009. Extensive dynamic thinning on the margins of the Greenland and Antarctic ice sheets. *Nature* 461, 971-975.
Rignot, E. 1998. Fast recession of a West Antarctic glacier. *Science*, 281(5376), 549–551, doi:10.1126/science.281.5376.549.

Rignot, E. 2001. Evidence for rapid retreat and mass loss of Thwaites Glacier, West Antarctica. *J. Glaciol.* **47**, 213–222.
Rignot, E. 2002. Ice-shelf changes in Pine Island Bay, Antarctica, 1947-2000. *J. Glac.* 48, 247–256.
Rignot, E.J. 2008. Changes in West Antarctic ice stream dynamics observed with ALOS PALSAR data. *Geophys. Res. Lett.* **35**, L12505, doi:10.1029/2008GL033365.
Rignot, E., J.L. Bamber, M.R. van den Broeke, C. David, Y. Li, W.J. van d Berg and E. van Meijgaard. 2008. Recent Antarctic ice mass loss from radar interferometry and regional climate modelling. *Nature Geosci.* 1, 106–110.
Sardeshmukh, P.D. and B.J. Hoskins. 1988. The generation of global rotational flow by steady idealized tropical divergence. *J. Atmos. Sci*. 45, 1228–1251.
Scherer, R.P., A Aldahan, S. Tulaczyk, G. Possnert, H. Engelhardt and B. Kamp. 1998. Pleistocene collapse of the West Antarctic Ice Sheet. *Science* 281, 82-85.
Schmeltz, M., E. Rignot, T.K. Dupont, D.R. Macayeal. 2002. Sensitivity of Pine Island Glacier, West Antarctica, to changes in ice-shelf and basal conditions: a model study. *J. Glaciol.* 48, 552-558.
Schneider, D. P. and E.J. Steig. 2008. Ice cores record significant 1940s Antarctic warmth related to tropical climate variability. *Proc. Natl Acad. Sci.* 105, 12154–12158.
Schneider, D.P., C. Deser, Y. Okumura. 2011. An assessment and interpretation of the observed warming of West Antarctica in the austral spring. *Clim. Dyn.* in press.
Schoof, C. 2007. Ice sheet grounding line dynamics: steady states, stability and hysteresis. *J. Geophys. Res.* 112(F03S28). doi:10.1029/2006JF000664
Scott, J., H. Gudmundsson, A. Smith, R.G. Bingham, H.D. Pritchard, and D.G. Vaughan. 2009. Increased rate of acceleration on Pine Island Glacier strongly coupled to changes in gravitational driving stress. Cyrosphere 3, 125–131.
Shepherd, A., D.J. Wingham and E.Rignot. 2004. Warm ocean is eroding West Antarctic ice sheet. *Geophys. Res. Lett.* 31, L23402.
Shepherd, A., D.J. Wingham, and J.A.D. Mansley. 2002. Inland thinning of the Amundsen Sea sector, West Antarctica. 2002. *Geophys. Res. Lett.* 29, doi:10.1029/2001GL014183.
Simmonds, I., and J. C. King. 2004. Global and hemispheric climate variations affecting the Southern Ocean. *Antarc. Sci*. 16(4), 401-413, doi:10.1017/S0954102004002226.
Smith, T.M., R.W. Reynolds, T.C. Peterson and J. Lawrimore. 2008. Improvements to NOAA's historical merged land–ocean surface temperature analysis (1880–2006). *J. Clim*. 21, 2283–2296.
Steig E.J., D.P. Schneider, S.D. Rutherford, M.E. Mann, J.C. Comiso and D.T. Shindell. 2009. Warming of the Antarctic ice sheet surface since the 1957 International Geophysical Year. *Nature* 457, 459-462.
Thoma, M., A. Jenkins, D. Holland, and S. Jacobs. 2008. Modelling Circumpolar Deep Water intrusions on the Amundsen Sea continental shelf, Antarctica. *Geophys. Res. Lett.*, **35**, L18602, doi:10.1029/2008GL034939.
Thompson, D.W.J. and S. Solomon. 2002. Interpretation of Recent Southern Hemisphere Climate Change. *Science* 296, 895–899.
Thomson, D.J. 1982. Spectrum estimation and harmonic analysis. *Proceed. IEEE*: 1055–1096.

Trenberth, K. 1984. Signal versus noise in the Southern Oscillation. *Mon. Weath. Rev.* 112: 326-332.

Turner, J. and 8 others. 2009. Non-annular atmospheric circulation change induced by stratospheric ozone depletion and its role in the recent increase of Antarctic sea ice extent. *Geophys. Res. Lett.* 36, L08502, doi:10.1029/2009GL037524.

Uppala, S. M. and 46 others. 2005. The ERA-40 re-analysis. *Q. J. R. Meteorol. Soc*. 131, 2961–3012.

van den Broeke, M. 2000. The semi-annual oscillation and Antarctic climate. Part 4: A note on sea ice cover in the Amundsen and Belling- shausen seas, *Int. J. Climatol.*, 20(4), 455–462.

Wingham D.J., A.J. Ridout, R. Scharroo, A.J. Arthern RJ and C.K. Schum CK. 1998. Antarctic elevation change from 1992 to 1996. *Science* 282:456–458

Wingham, D.J., D.W. Wallis and A. Shepherd, 2009. A spatial and temporal evolution of Pine Island Glacier thinning, 1995–2006. *Geophys. Res. Lett.* 36, (2009).

Wingham, D.J., D.W. Wallis, and A. Shepherd. 2009. Spatial and temporal evolution of Pine Island Glacier thinning, 1995–2006. *Geophys. Res. Lett.* 36, L17501, doi:10.1029/2009GL039126.

FIGURE CAPTIONS

Figure 1. a) Climatological sea level pressure (hPa) for June-July-August over the Amundsen and Bellingshausen Seas, with outline of the continent in blue. Red box shows the location (70°S, 100° to 125° W) centered on the continental slope used for the zonal wind stress. Dashed box denotes the Amundsen Sea Embayment. **b**) Monthly zonal wind stress and **c)** daily climatological wind stress from ERA40/ERA-interim 1979-2009. Positive values are westerly.

Figure 2. Relationship between westerly wind stress over the continental slope and CDW layer thickness on the inner shelf in the Amundsen Sea Embayment. **a**) Correlation of monthly anomalies (mean seasonal cycle removed) of zonal wind stress with CDW layer thickness (layers 7 and 8 from Thoma and others, 2008), for December 1979 through November 2004. **b**) Spectral coherence between wind stress and CDW inner shelf layer thickness as a function of period. Dashed line shows 95% confidence limit. **c**) Phase of the coherence estimates, with 95% uncertainties (shading). Dashed line shows phase for a constant 2.5-month lead of wind stress over CDW changes. Spectral coherence and phase calculated using the Thomson multi-taper method with a bandwidth of ~0.6/yr. In each figure, thin lines are NCEP2 data, thick lines are ERA40/interim data.

Figure 3. Variations in thickness of CDW layers (layers 7 and 8) on the contintental slope (dashed) and inner continental shelf (solid) from Thoma and others (2008). **a**) Monthly averages from 1980 to 2004. **b**) Seasonal climatology for the period 1990-1999. **c**) Seasonal climatology for the period 1980-1989. **d**) The difference in between b) and c).

Figure 4. Seasonal wind stress climatology from NCEP2 (dashed) and ERA40 (solid) for **a)** 1990-1999 **b**) 1980-1989, and **c)** their difference. Although the mean wind stress maximum occurs in the same seasons in both periods (winter and spring), the seasonal mean westerly wind stress more than doubled in the fall between the 1980s and the 1990s.

Figure 5. Correlation between zonal wind stress in the Amundsen Sea Embayment region (red box in Figure 1) in austral fall (MAM) **a)** sea level pressure, **b)** upper troposphere (200 hPa) stream function and **c)** sea surface temperature. Data are from ERA40/interim and ERSST3 (Smith and others, 2008) for the period 1979-2009. Areas of statistically significant correlation are shaded (~0.35 corresponds to 95% confidence level).

Figure 6. Change in **a)** sea level pressure (SLP), **b)** upper troposphere (200 hPa) stream function (Z200) and **c)** sea surface temperature (SST) variations in austral fall (MAM) between 1980-1989 and 1990-1999 from ERA40/interim and ERSST3 data.

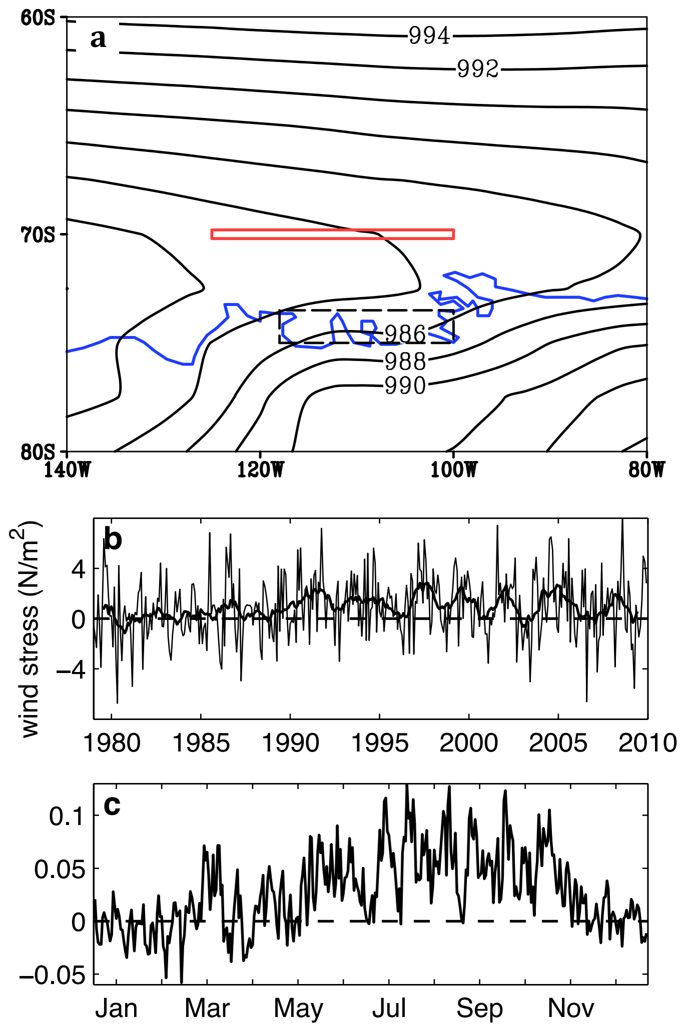

Figure 1. a) Climatological sea level pressure (hPa) for June-July-August over the Amundsen and Bellingshausen Seas, with outline of the continent in blue. Red box shows the location (70°S, 100° to 125° W) centered on the continental slope used for the zonal winds stress. Dashed box denotes the Amundsen Sea Embayment. **b**) Monthly zonal wind stress and **c)** daily climatological wind stress from ERA40/ERA-interim 1979-2009. Positive values are westerly.

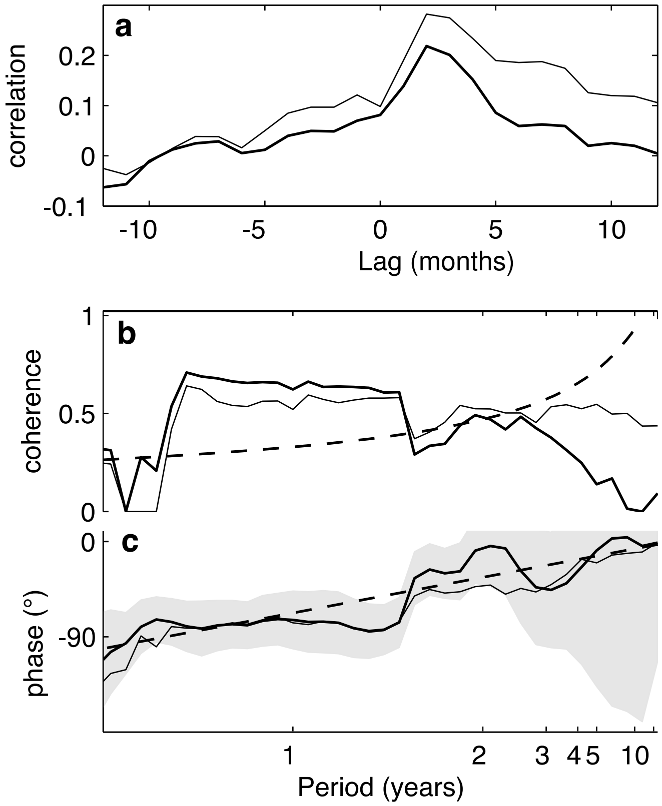

Figure 2. Relationship between westerly wind stress at the shelf edge and Circumpolar Deep Water layer thickness on the inner shelf in the Amundsen Sea Embayment. **a**) Correlation of monthly anomalies (mean seasonal cycle removed) of zonal wind stress with CDW layer thickness (layers 7 and 8 from Thoma and others, 2008), for December 1979 through November 2004. **b**) Spectral coherence between wind stress and CDW inner shelf layer thickness as a function of period. Dashed line show 95% confidence limit. **c**) Phase of the coherence estimates, with 95% uncertainties (shading). Dashed line shows phase for a constant 2.5-month lead of wind stress over CDW changes. Spectral coherence and phase calculated using the Thomson (1982) multi-taper method with a bandwidth of ~0.6/yr. In each figure, thin lines are NCEP2 data, thick lines are ERA40/interim data.

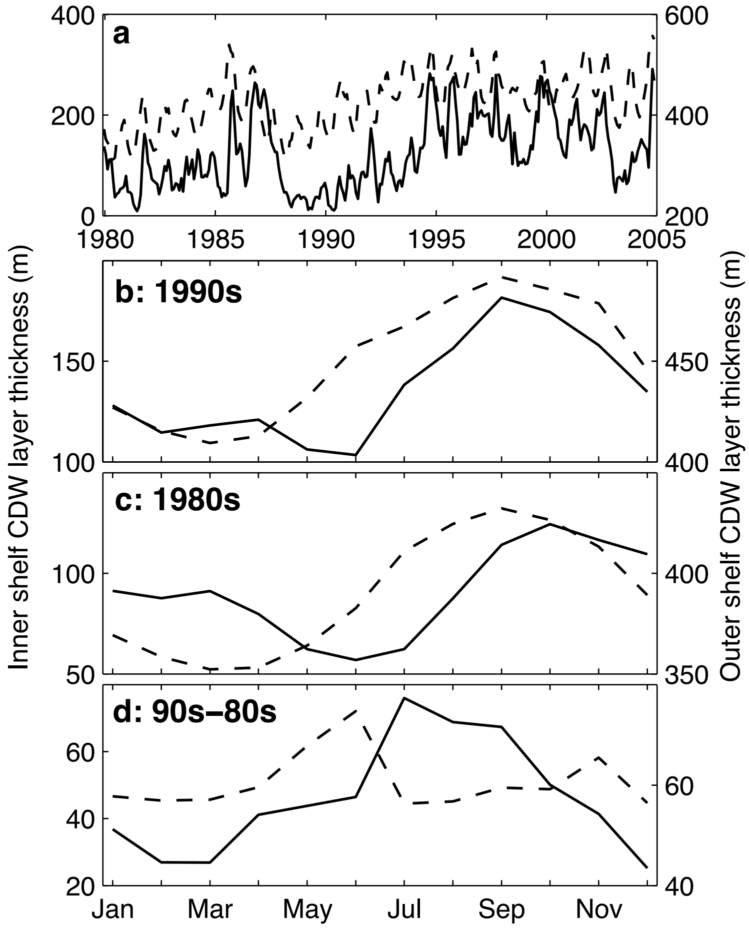

Figure 3. Variations in thickness of Circumpolar Deep Water layers (layer 7 and 8) on the outer shelf slope (dashed) and inner continental shelf (solid) from Thoma and others (2008). **a**) monthly averages from 1980 to 2004. **b**) seasonal climatology for the period 1980-1989, **c**) for 1990-1999, and **d**) their difference.

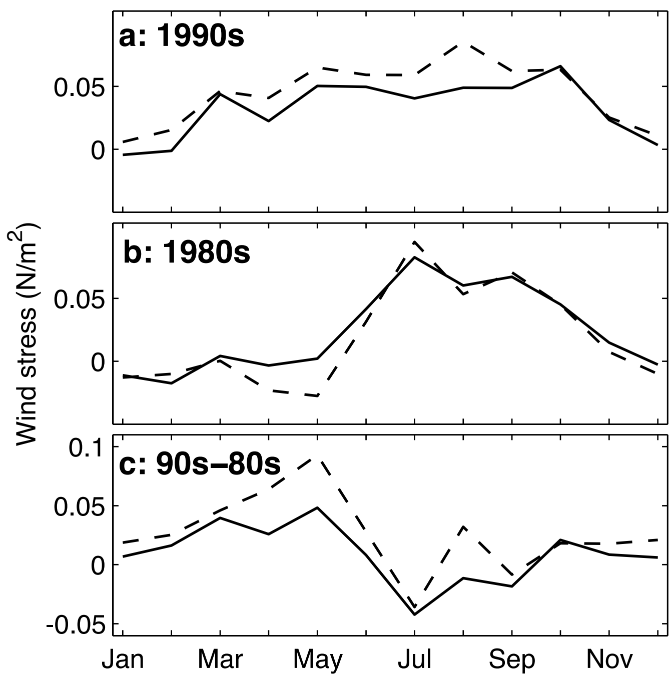

Figure 4. Monthly wind stress climatology from NCEP2 (dashed) and ERA40 (solid) for **a)** 1990-1999 **b**) 1980-1989, and **c)** their difference. Although the mean wind stress maximum occurs in the same seasons in both periods (winter and spring), the seasonal mean westerly wind stress more than doubled in the fall between the 1980s and the 1990s.

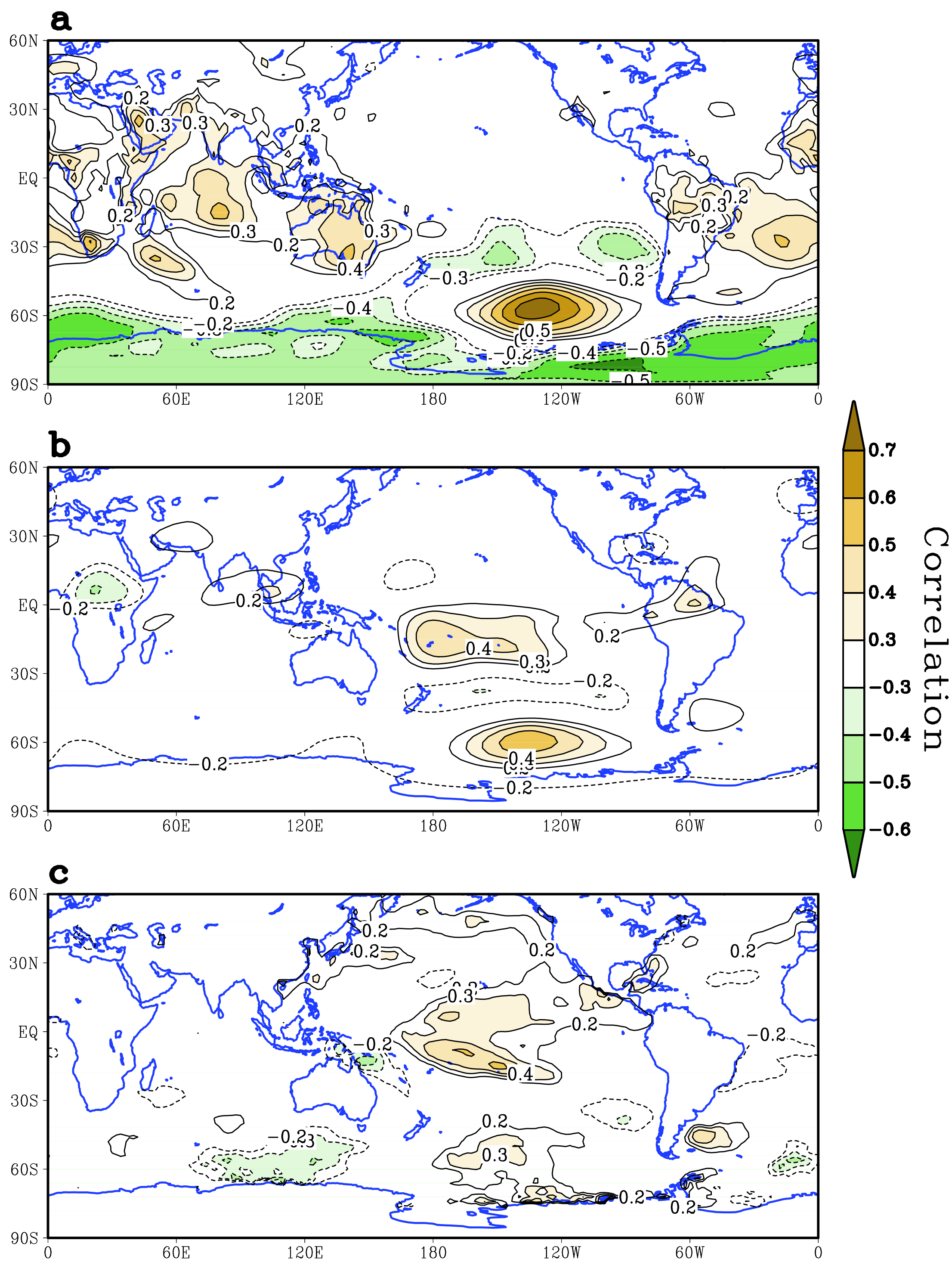

Figure 5. Correlation between zonal wind stress in the Amundsen Sea Embayment region (red box in Figure 1) in austral fall (MAM) **a)** sea level pressure, **b)** upper troposphere (200 hPa) stream function and **c)** sea surface temperature. Data are from ERA40/interim and ERSST3 (Smith and others, 2008) for the period 1979-2009. Areas of statistically significant correlation are shaded (~0.35 corresponds to 95% confidence level).

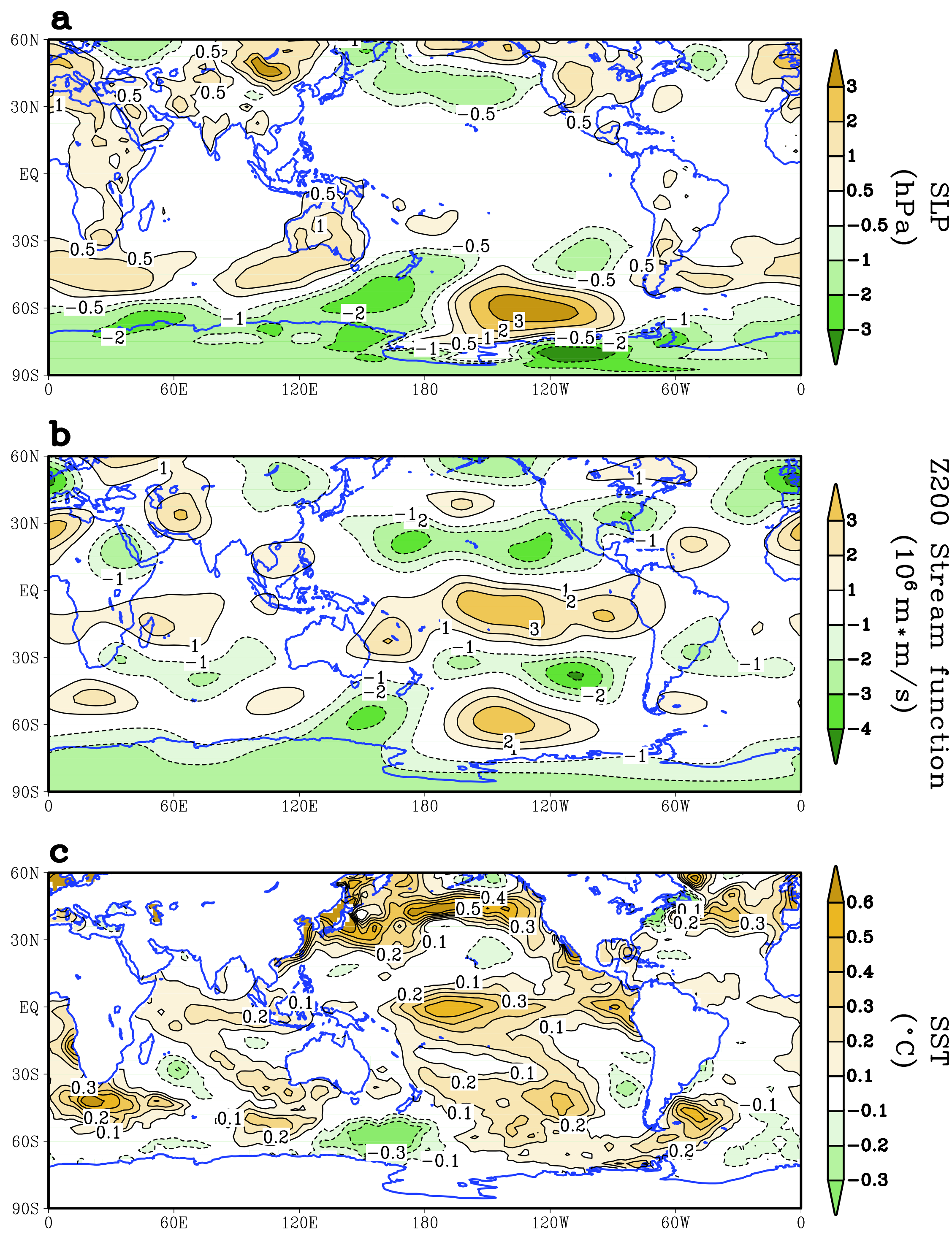

Figure 6. Change in **a)** sea level pressure (SLP), **b)** upper troposphere (200 hPa) stream function (Z200) and **c)** sea surface temperature (SST) variations in austral fall (MAM) between 1980-1989 and 1990-1999 from ERA40/interim and ERSST3 data.